# Slip Modulus of Screws in Timber and Lightweight Concrete Composite Structures

Ljiljana Kozarić, Danijel Kukaras,* Aleksandar Prokić, Miroslav Bešević, and Milan Kekanović

The use of lightweight concrete in timber-concrete composite structures for the purposes of reconstruction, upgrading, and strengthening has increasing application potential. The correct combination of mechanical properties of both materials can preserve the beneficial aspects of timber in tension and concrete in compression, while reducing the weight of the structure. This paper experimentally evaluated the slip modulus of screw connectors as one of the key issues in the structural design of these types of composite structures. The results of four groups of push-out tests, which were performed on composite samples, are presented. All of the samples had identical cross sections, but each group was made with a different lightweight concrete density class according to Eurocode 2. The obtained results were compared with the values recommended by Eurocode 5. The analysis showed that the code recommendations yielded slip modulus values that were considerably higher than the ones obtained experimentally, which could lead to unsafe timber and lightweight concrete structures.

*Keywords: Timber; Lightweight concrete; Composite structure; Slip modulus; Push-out test*

*Contact information: Faculty of Civil Engineering Subotica, University of Novi Sad, Kozaracka 2a, Subotica, 24000, Serbia; *Corresponding author: danijel.kukaras@gmail.com*

## INTRODUCTION

The first officially recorded technical document that describes timber-concrete composite structures dates back almost 100 years and is the German patent DE 334431 C submitted in 1919 and approved in 1921 under the title "Decke aus hochkantig stehenden Holzbohlen oder Holzbrettern und Betondeckschicht (Floor structure constructed from wooden planks or wooden boards with concrete slab)" (Mueller 1921). Interest in these types of structures is primarily motivated by the optimal structural performance and construction costs (Yeoh *et al*. 2011). When compared with classic steel-concrete composite structures, timber-concrete composite (TCC) structures have a reduced weight and maintain a reasonable bearing capacity. The natural property of timber being a $CO_2$ sink rather than a $CO_2$ source makes it favorable in light of worldwide efforts to reduce greenhouse gas emissions.

With this in mind, the use of lightweight aggregate concrete (LWAC) can increase the benefits of wider use of TCC structure by further improving the structural performance, energy efficiency, and insulation of sound, temperature, and fire, all of which can be achieved alongside a further reduction in the weight of the structure (Kekanović *et al*. 2014).

The use of composite floor slabs made from timber and lightweight aggregate concrete (TLCC) is not widespread. Most probably, this is the result of a lack of guidelines within current codes that define the specific use of LWAC within timber-concrete composite structures. This creates an opportunity for research efforts to be aimed at practical applications of these types of structures in building construction.

For classic TCCs, the effectiveness of the TLCC system is largely dependent upon the properties of the concrete-timber interlayer because it has a major influence on the structural response. Girders made with TCC and mechanical fasteners show a certain amount of slip in this interlayer when an external load is applied. This makes choosing the fastener an important decision during the design process. It is crucial to determine the load-slip behavior of the concrete-timber interlayer to make reliable predictions regarding the behavior of the structure under external loading. The amount of slip depends on the type of applied fasteners, their spacing, shape, installation method, and other factors. When glue is used as the fastening method, the interlayer is considered to be stiff, which means the joint between the timber and concrete is fixed, the cross section can be designed as uniform, and the no-slip calculation theory can be applied. The design is then reduced to the classic design approach that is used for uniform cross sections. In contrast, when mechanical fasteners are used, a partial joining of the material is observed and the structural design in these cases has to take into account the load-slip behavior within the concrete-timber interlayer. Current design practices use a definition of the slip modulus that is based on the load-slip curve to calculate the deformation of TCC structures.

Mechanical fasteners show nonlinear load-slip behavior (He *et al.* 2016; Xie *et al*. 2017), and so deformation calculations have to include several slip modulus values in the structural design. Ceccotti (1995) proposed two values: $K_{ser}$ for the serviceability limit state and $K_u$ for the ultimate limit state. The slip modulus $K_{ser}$ is defined as the secant modulus at 40% of the failure load, while $K_u$ is defined as the secant modulus at 60% of the failure or maximum load.

In general, the slip modulus values are determined by experimental analysis according to the standard EN 26891 (1991) for joints made with mechanical fasteners in timber structures. According to this standard, the maximum load is defined as either the force at which the sample reaches failure/destruction or the force at which the slip reaches a value of 15 mm. With this in mind, $K_{ser}$ used for the serviceability limit state is defined as the secant at 0.4 $F_{est}$, where $F_{est}$ represents an estimation of the failure force.

However, according to EN 1995-1-1 (2004) for the serviceability limit state, it is specified that the $K_{ser}$ for timber-concrete joints is to be calculated on the basis of the wood density of timber-timber joints with dowels, bolts, and pre-drilled nails, and this value may be multiplied by 2. This value, expressed in N/mm, is calculated with Eq. 1,

$$K_{ser} = \rho_m^{1.5} \frac{d}{23} \tag{1}$$

where $\rho_m$ is the volumetric density of the timber element (kg/m$^3$) and $d$ is the diameter of the fastener (mm).

When used for validation of the ultimate limit state, the joint slip modulus ($K_u$) is equal to (2/3)$K_{ser}$, according to EN 1995-1-1 (2004).

Recent experimental studies have shown that the proposed method for the determination of the joint slip modulus in EN 1995-1-1 (2004) is practical, but it is oversimplified and does not take into account the diversity of contemporary solutions for joint creations within these types of composite structures. For example, by comparing the analytical results obtained using EN 1995-1-1 (2004) with experimental results, Ceccotti *et al*. (2007) determined that the slip modulus of glued fasteners provided experimentally is considerably higher. The experimental values of the slip modulus were up to 50% lower than those obtained according to EN 1995-1-1 (2004).

Within this paper, the slip modulus of the composite timber-lightweight concrete joint was determined experimentally for four weight classes of LWAC. The composite action of the timber and lightweight concrete was achieved by means of vertical screws (Fig. 1). This type of connection was chosen because it represents the most widely used and cost-efficient method that is easy to implement and does not rely heavily on the skill level of the labor force. The experimentally obtained results were compared with the results obtained from EN 1995-1-1 (2004).

## EXPERIMENTAL

### Materials and Methods

Four model types were chosen for this analysis, which corresponded to typical floor slabs made with the TCC solution that was investigated previously by Kozarić (2015). All of the models had identical geometric properties and fasteners. The weight class of the LWAC was varied. A short overview of the models and concrete weight classes according to EN 1992-1-1 (2004), as well as the mixtures per cubic meter of lightweight concrete, is given in Table 1. The concrete mixtures consisted of ground expanded polystyrene (EPS) (Kekanović *et al.* 2014), Portland cement (class 42.5), aggregate (size = 0 mm to 4 mm), water, and synthetic polypropylene fibers (length = 6 mm) (SIKA AG, Baar, Switzerland).

**Table 1.** Weight Class and Compressive Strength of the Applied LWAC

| Mo-del | Aggreg. Weight Class | EPS $m_s$ | Cement $m_c$ | Aggregate $m_a$ | Water $m_w$ | Fibers $m_f$ | Compress. Strength $f_c$ | Elastic. modulus $E$ |
|---|---|---|---|---|---|---|---|---|
| Unit | - | kg/m$^3$ | kg/m$^3$ | kg/m$^3$ | kg/m$^3$ | kg/m$^3$ | N/mm$^2$ | GPa |
| G1 | 1.2 | 9.50 | 425 | 800 | 240 | 1.00 | 6.76 | 7.11 |
| G2 | 1.4 | 8.00 | 425 | 1050 | 240 | 1.00 | 8.96 | 9.35 |
| G3 | 1.6 | 6.00 | 500 | 1000 | 200 | 1.00 | 16.17 | 14.40 |
| G4 | 1.8 | 4.40 | 525 | 1030 | 210 | 1.00 | 23.48 | 15.68 |
| Note: Variables $m_s$, $m_c$, $m_a$, $m_w$, and $m_f$ represent a mass per m$^3$ of the mixture, for EPS, cement, aggregate, water and fibers, respectively. | | | | | | | | |

The models were made from fir beams (*Abies alba*). The fir wood was acquired from the Austrian company Holzhof-Schmidt GmbH (Aspangberg-St.Peter, Austria) with a certificate of strength for class C16. The mean wood density ($\rho_m$) was determined using samples that were taken from the same batch of timber that was used in the experimental study and was found to be 383.5 kg/m$^3$. The mean moisture content of the samples was 11.8%. According to the EN 408:2010, experimental determination of the modulus of elasticity in bending and bending stiffness for the chosen timber yielded values of 9.12 GPa and 17.21 MPa, respectively.

Joining of the timber beam and concrete slab was achieved with typical lag screws that had a diameter of 10 mm and a length of 150 mm (Fig. 1). The screws were installed perpendicular to the longitudinal axes of the timber beam with a spacing of 20 cm. Ten centimeters of their length were embedded into the wood, while 5 cm were left to be anchored in the concrete.

The relative ratio of the elasticity modulus of the LWAC with aggregate weight class (AWC) of 1.4 and the chosen timber has value close to 1.0. This ratio is lower for AWC 1.2 and higher for AWC 1.6 and 1.8. The lag screws used for this experiment were standard product and their mechanical properties correspond to steel hex-wood screws according to the DIN 571 standard, *i.e.* considerably higher than mechanical properties of LWAC and timber.

Because there are no specific standards for composite structures made from timber and lightweight concrete, the slip modulus was determined based on the models and procedures stipulated in EN 1995-1-1 (2004). Similar models were investigated by Stevanović (2004). The geometry and shape of the proposed models proved to be simple for construction and reliable with respect to the obtained results and their application.


**Fig. 1.** (a) Lag screw used for slip modulus testing/evaluation; (b) spacing of the screws; and (c) timber beam covered with PVC foil

A partial depiction of the sample production is presented in Fig. 2. The dimensions and description of the samples are given in Fig. 3. In total, 12 samples for the experimental evaluation of the slip modulus were produced (Fig. 2). There were three samples for each model, which are described in Table 1.


**Fig. 2.** (a) Detail of a sample prior to concrete casting; (b) casting of the concrete; and (c) all 12 samples ready for testing

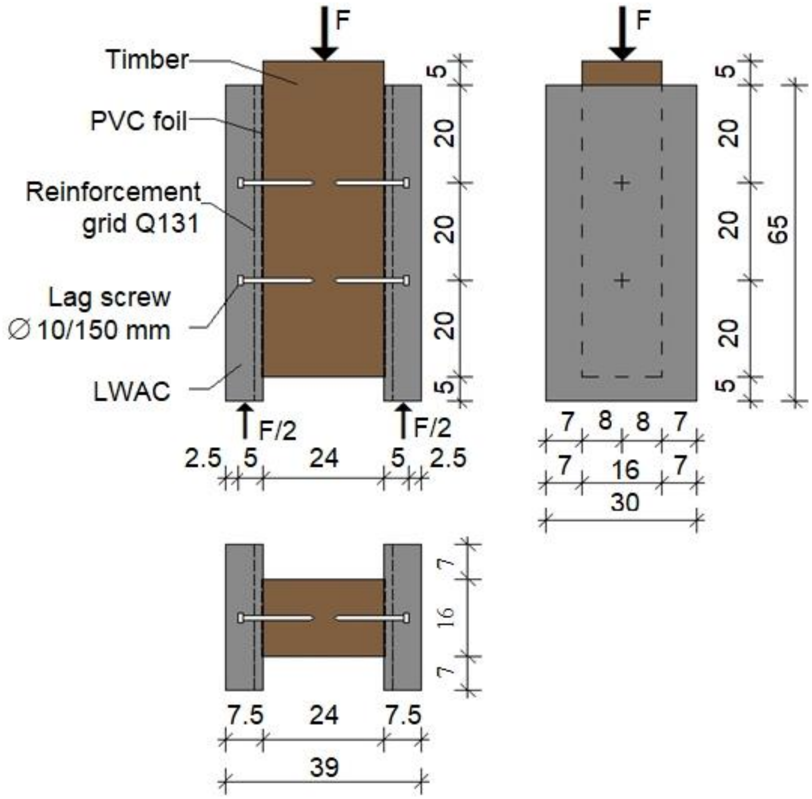


**Fig. 3.** Shape and dimensions of the samples for the slip modulus evaluation. Dimensions are shown in cm.

Testing of the samples was conducted according to EN 26891 (1991). The force was applied to a timber section of the sample using a 20-mm steel pad that was placed over the whole upper timber surface to ensure uniform load transfer. The concrete section of the sample rested on the horizontal steel plate of the compression tester. The force was applied with a universal testing machine (P-250, Milaform-Service, Neftekamsk, Russia). The applied force was monitored with a 200-kN compression load cell (0.02% precision) (CZL110D, SAH Electronics, Belgrade, Serbia) and weighing batching controller (LH8-IRRD, SAH Electronics). The deformation/slip on the surface between the timber and concrete was measured with digital calipers (MIB Messzeuge GMBH, Spangenberg, Germany) with a maximum deflection range of 150 mm and 0.01-mm reading. Simultaneous data acquisition from the load cell and digital calipers (Szegedi *et al*. 2015) was conducted at a rate of 4 Hz (Caliper Data Acquisition System, Su-Tech, Subotica, Serbia). Each sample was equipped with four calipers, two on each side of the sample, in the vicinity of the joint surface between the timber and concrete to maximize the precision of the measurements (Fig. 4). The measurements were taken from the middle of the sample height, which corresponded to the middle of the spacing between the screws. The body of each caliper was fixed to the timber beam, while its bottom tip was positioned on the steel bracket that was glued to the concrete (Fig. 4).

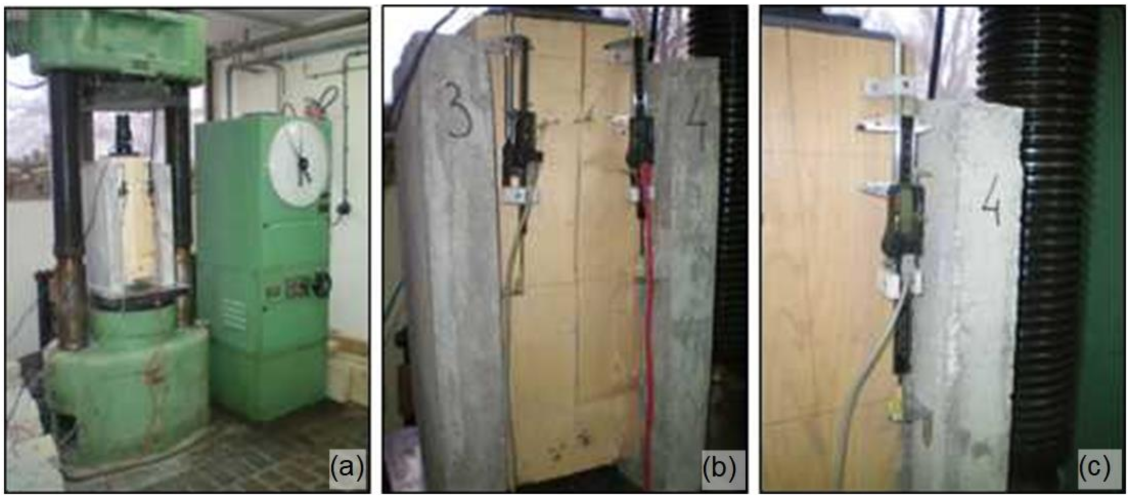


**Fig. 4.** (a) Sample during testing and (b and c) position of the calipers relative to the sample

The load was applied according to the procedure given in EN 26891 (1991). Initially, for each sample, the estimated maximum load was determined, and the application of 40% of this load was applied over 2 min. This was followed by a constant load level for 30 s, and then the sample was unloaded over 1.5 min until 10% of the estimated maximum load was achieved. This load was kept constant for 30 s, and then a final loading of the sample took place until failure occurred or a maximum displacement of 15 mm was measured (Fig. 5). The total testing time for each sample was approximately 10 min. After completing the first sample of each model, the remaining two samples were tested according to the same procedure, but the initially estimated maximum load value was replaced with the maximum load value recorded during the testing of the first sample.

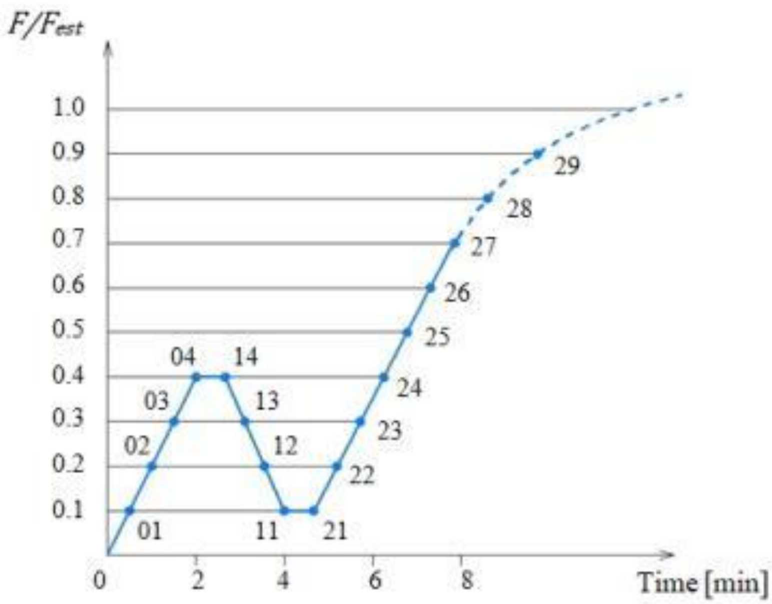


**Fig. 5.** Procedure for the application of force according to EN 26891 (1991)

## RESULTS AND DISCUSSION

For the tested samples, the following diagrams of force *vs*. displacement ($F$-$\delta$) were obtained (Figs. 6 and 7).

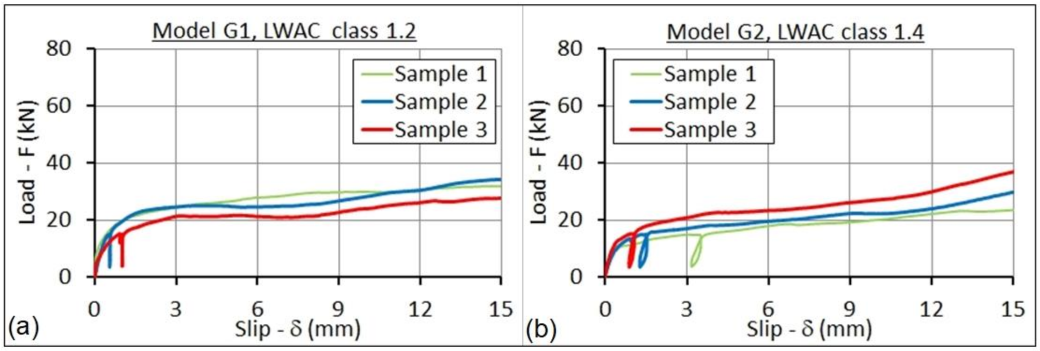


**Fig. 6.** Load-slip ($F$-$\delta$) curves for test groups G1 (a) and G2 (b)

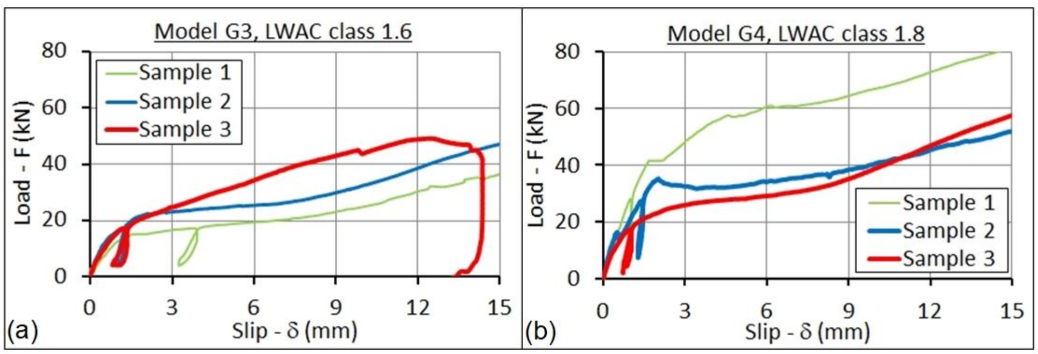


**Fig. 7.** Load-slip ($F$-$\delta$) curves for test groups G3 (a) and G4 (b)

The experimental investigations of the timber-lightweight concrete joints showed that the load-slip curves were not linear. The fact that the $F$-$\delta$ diagrams were not linear consequently revealed that the slip modulus was also not linear and that it was different for practically each load step.

According to EN 26891 (1991), the determination of the slip modulus $K_{ser}$ is defined as the secant modulus at 0.4 $F_{est}$,

$$K_{ser} = \frac{0,4F_{est}}{n}\frac{1}{\delta_{i,mod}} \tag{2}$$

$$\delta_{i,mod} = \frac{4}{3}\left(\delta_{04} - \delta_{01}\right) \tag{3}$$

where $n$ is the number of connectors, $\delta_{i,mod}$ is the modified displacement (mm), obtained with Eq. 3, $\delta_{04}$ is the displacement (mm) measured at $0.4F_{est}$, and $\delta_{01}$ is the displacement (mm) measured at 0.1 $F_{est}$.

Verification of the load bearing capacity was obtained by assuming a slip modulus where $K_u$ is $(2/3)K_{ser}$. For the calculation of the slip modulus, the $F_{est}$ was corrected and replaced with the maximum force ($F_{max}$), which is a standard procedure, provided that it showed a more than 20% difference from the $F_{est}$. In this case, the displacements $\delta_{04}$ and $\delta_{01}$ were taken from the $F$-$\delta$ diagrams and evaluated against the corrected value of the $F_{est}$, *i.e.* $F_{max}$. The maximum load during the experimental testing was either the load registered at failure or a displacement/slip of 15 mm.

Based on the aforementioned methodology of the slip modulus determination and with the use of the $F$-$\delta$ diagrams, the $K_{ser}$ was determined for 0.4 $F_{est}$, and the median values were determined for each model (G1, G2, G3, and G4). These values are given in Tables 2 and 3.

**Table 2.** Test Results for All Specimens

| Model | Sample | $F_{max}$ (kN) | $\delta_{max}$ (mm) | 0.4 $F_{max}$ (kN) | $\delta_{04}$ (mm) | $\delta_{01}$ (mm) | $\delta_{i,mod}$ (mm) | $K_{ser}$ (kN/mm) |
|---|---|---|---|---|---|---|---|---|
| G1 | 1.2/1* | 31.81* | 15.0* | 3.18* | 0.25* | 0.01* | 0.24* | - |
| | 1.2/2 | 34.10 | 15.0 | 3.74 | 0.55 | 0.07 | 0.64 | 5.33 |
| | 1.2/3 | 27.71 | 15.0 | 2.77 | 0.42 | 0.01 | 0.55 | 5.07 |
| G2 | 1.4/1* | 23.44* | 15.0* | 2.34* | 0.38* | 0.06* | 0.43* | - |
| | 1.4/2 | 29.71 | 15.0 | 2.97 | 0.62 | 0.01 | 0.81 | 3.65 |
| | 1.4/3 | 36.88 | 15.0 | 3.77 | 1.00 | 0.05 | 1.27 | 2.91 |
| G3 | 1.6/1* | 36.57* | 15.0* | 4.33* | 3.84* | 0.26* | 4.77* | - |
| | 1.6/2 | 47.12 | 15.0 | 4.31 | 1.20 | 0.13 | 1.43 | 3.30 |
| | 1.6/3 | 45.07 | 14.2 | 4.34 | 1.30 | 0.14 | 1.55 | 2.91 |
| G4 | 1.8/1* | 81.42* | 15.0* | 6,96* | 1.01* | 0.20* | 1.08* | - |
| | 1.8/2 | 51.93 | 15.0 | 5.9 | 0.98 | 0.10 | 1.17 | 4.43 |
| | 1.8/3 | 57.52 | 15.0 | 5.75 | 1.96 | 0.18 | 2.37 | 2.42 |
| Values marked with an asterisk (*) are the values obtained from the first sample that was used to evaluate the $F_{est}$ according to EN 26891 (1991) | | | | | | | | |

**Table 3.** Slip Modulus Obtained from the Tests According to Eurocode 5

| Model | $K_{ser,mean}$ (kN/mm) | $K_{ser, EC5}$ (kN/mm) | $K_{u,mean}$ (kN/mm) | $K_{u, EC5}$ (kN/mm) |
|---|---|---|---|---|
| G1 | 5.20 | 6.53 (3.27) | 3.47 | 4.35 (2.18) |
| G2 | 3.28 | | 2.19 | |
| G3 | 3.11 | | 2.07 | |
| G4 | 3.42 | | 2.28 | |
| Values in parentheses for $K_{ser, EC5}$ and $K_{u, EC5}$ are the values calculated by applying the Eurocode 5 recommendation based on the mean density of the wood and timber-timber joints with dowels, bolts, and pre-drilled nails multiplied by 1. The values above those were obtained in the same manner, but were instead multiplied by 2. | | | | |

The stiffness of the joint ($k$) represents the relationship between the slip modulus ($K$) and the distance between the connectors ($s$) ($k = K/s$) (Demarzo and Tacitano 2000). Within the experimental work presented in this paper, the connectors were installed at an equidistance of 20 cm. The calculated values of the joint stiffness for all four models are given in Table 4.

**Table 4.** Stiffness of the Joint for the Tested Models

<table>
<tr><th>Model</th><th>$k_{ser}$ (MPa)</th><th>$k_{ser,EC5}$ (MPa)</th><th>$k_u$ (MPa)</th><th>$k_{u,EC5}$ (MPa)</th></tr>
<tr><td>G1</td><td>26.00</td><td rowspan="4">32.65 (16.35)</td><td>17.35</td><td rowspan="4">21.75 (10.90)</td></tr>
<tr><td>G2</td><td>16.40</td><td>10.95</td></tr>
<tr><td>G3</td><td>15.55</td><td>10.35</td></tr>
<tr><td>G4</td><td>17.10</td><td>11.40</td></tr>
<tr><td></td><td colspan="2">Serviceability limit state joint stiffness<br>$k_{ser}$ - measured mean values<br>$k_{ser,EC5}$ - values calculated from EC5</td><td colspan="2">Ultimate limit state joint stiffness<br>$k_u$ - measured mean values<br>$k_{u,EC5}$ - values calculated from EC5</td></tr>
</table>

Subsequent analysis of the failure modes of the samples revealed that strength ratios between the concrete and timber played a significant role. Samples with AWC 1.2 and 1.4 showed failure mode with rotation (He *et al.* 2016), (Fig. 8), while samples with AWC 1.6 and 1.8 showed failure mode hinge that appeared in the LWAC, (Fig. 9). The overall type of failure for all samples was ductile, consisting of a single plastic deformation without sudden propagation. Observed modes of failure indicate that their shape depends on the concrete strength which, in the case of LWAC, can be lower than that of the timber.

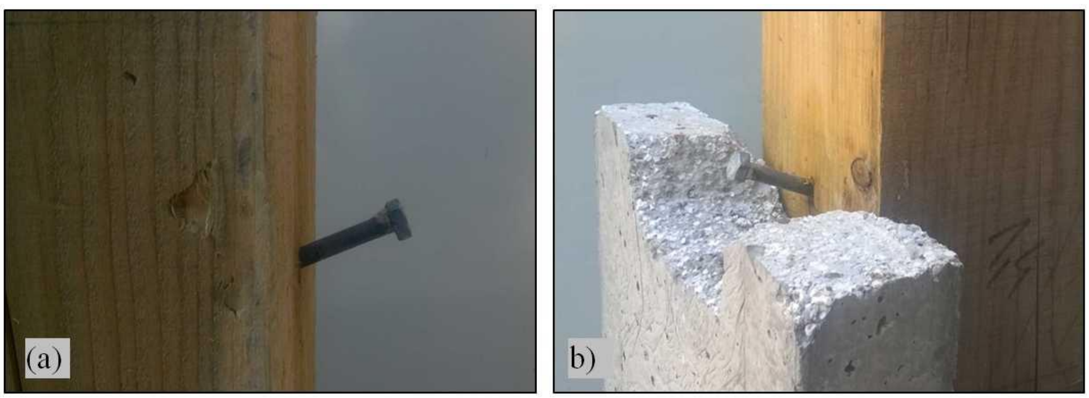


**Fig. 8.** Failure modes for the timber - LWAC (a) AWC 1.2 and (b) AWC 1.4

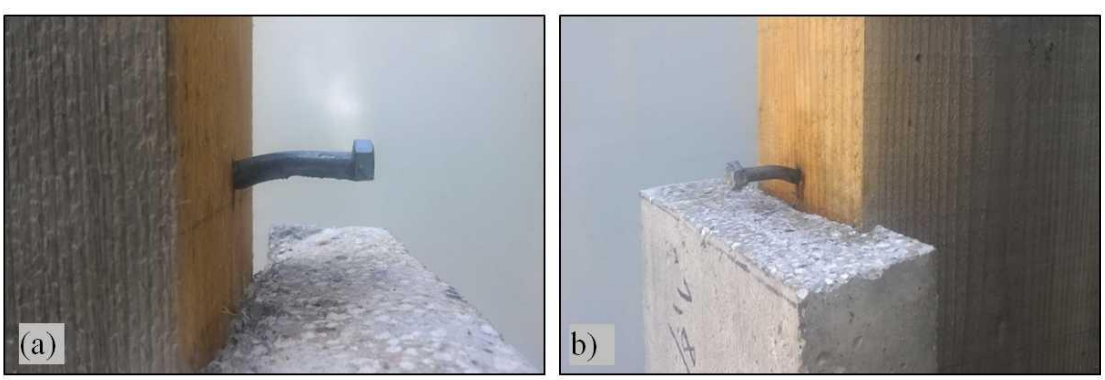


**Fig. 9.** Failure modes for the timber - LWAC (a) AWC 1.6 and (b) AWC 1.8

The analysis of the obtained results showed that the experimentally determined slip modulus for the tested models varied depending on the class of the lightweight concrete. In general, the maximum load for all of the samples increased as the density of the lightweight concrete increased as was expected, while the slip modulus decreased when the concrete class changed from 1.2 to 1.4 and slightly increased when the class changed from 1.6 to 1.8 (Fig. 10). This behavior could not be observed if only the code recommendation was used, where the calculated joint stiffness for the tested model was 32.65 MPa for the serviceability limit state and 21.75 MPa for the ultimate limit state, regardless of the LWAC class. The tests conducted showed that where the use of LWAC within TLCC structures is concerned, the slip modulus expressions should be modified to include the properties of the LWAC. These results can motivate further research that will include more TLCC samples with different LWAC classes and mechanical properties, which would enable more precise recommendations for the slip modulus in these types of structures, and thus clear the way for their wider use.

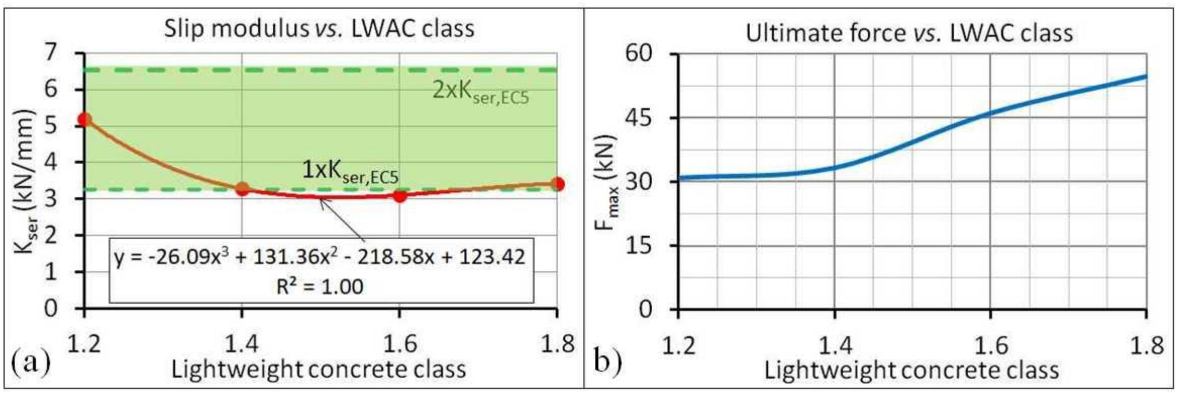


**Fig. 10.** Dependence of the slip modulus (a) and ultimate force (maximum load) (b) on the lightweight concrete class for all of the tested samples

## CONCLUSIONS

1. The slip modulus and joint stiffness were considerably lower than the values that were obtained by applying the recommendations in EN 1995-1-1 (2004).
2. The experimentally obtained values and calculated values varied by 25% for the LWAC class 1.2 and by approximately 50% for the LWAC classes 1.6 and 1.8
3. The code recommendations for the slip modulus appeared to be overestimated for TLCC structures. In EN 1995-1-1 (2004), the slip modulus is defined for TCC structures with normal concrete, where it is expected that the timber beam behavior will be the governing factor when it comes to the concrete-timber interlayer. However, in the case of TLCC structures, this experimental study showed that the slip behavior can be governed by the LWAC as well and depends on the LWAC class and mechanical properties.

4. The presented experimental research showed that for LWAC classes 1.4 and 1.6 the load-slip behavior and failure of the joint can be governed by both the properties of the timber and LWAC because of their similar mechanical properties. The slip modulus for the LWAC with a higher compressive strength (LWAC class 1.8 in this paper), while still lower than the code recommendation, showed a gradual increase, which made it closer to the values in the code recommendations.

## ACKNOWLEDGMENTS

This research was partly funded by the Faculty of Civil Engineering in Subotica pursuant to Clause 23 in “Guidelines for transfer of knowledge and cooperation with the industry”.

## REFERENCES CITED

Ceccotti, A. (1995). "Timber-concrete composite structures," in: *Timber Engineering STEP 2: Design – Details and Structural Systems*, H. J. Blass (ed.), Centrum Hout, Zaandam, The Netherlands.
Ceccotti, A., Fragiacomo, M., and Giordano, S. (2007). "Long-term and collapse tests on a timber-concrete composite beam with glued-in collection," *Mater. Struct.* 40(1), 15-25. DOI: 10.1617/s11527-006-9094-z
EN 1992-1-1 (2004). "Eurocode 2: Design of concrete structures - Part 1-1: General rules and rules for buildings," European Committee for Standardization, Brussels, Belgium.
EN 1995-1-1 (2004). "Eurocode 5: Design of timber structures - Part 1-1: General - Common rules and rules for buildings," European Committee for Standardization, Brussels, Belgium.
EN 26891 (1991). "Timber structures - Joints made with mechanical fasteners - General principles for the determination of strength and deformation characteristics," European Committee for Standardization, Brussels, Belgium.
Demarzo, M. A., and Tacitano, M. (2000). "Semirigid composite wood-concrete T-beams," World Conference on Timber Engineering, Whistler Resort, British Columbia, Canada.
He, G., Xie, L., Wang, X., Yi, J., Peng, L., Chen, Z., Gustafsson, P. J., and Crocetti, R. (2016). "Shear behavior study on timber-concrete composite structures with bolts," *BioResources* 11(4), 9205-9218. DOI: 10.15376/biores.11.4.9205-9218
Kekanović, M., Kukaras, D., Čeh, A., and Karaman, G. (2014). "Lightweight concrete with recycled ground expanded polystyrene aggregate," *Technical Gazette* 21(2), 309-315.
Kozarić, L. (2015). "Vibrations of repaired wooden floors caused by human action," *Wood Res.-Slovakia* 60(4), 663-670.
Mueller, P. (1921). “Decke aus hochkantig stehenden Holzbohlen oder Holzbrettern und Betondeckschicht (Floor structure constructed from wooden planks or wooden boards with concrete slab),” German Patent DE 334431 C.
Stevanović, B. (2004). "Experimental and theoretical analysis of timber: Concrete composite beams with mechanical connectors," *Mater. Struct.* 47(1-2), 29-46.
Szegedi, A., Szegedi, M., and Kukaras, D. (2015). "Universal data logger for electronic

measurement devices," in: *Proceedings of the International Conference Contemporary Achievements in Civil Engineering*, Subotica, Serbia.

Xie, L., He, G., Wang, A., Gustafsson, P. J., Crocetti, R., Chen, L., Li, L., and Xie, W. (2017). "Shear capacity of stud-groove connector in glulam-concrete composite structure," *BioResources* 12(3), 4690-4706. DOI: 10.15376/biores.12.3.4960-4706

Yeoh, D., Fragiacomo, M., De Franceschi, M., and Boon, K. H. (2011). "State of the art on timber-concrete composite structures: Literature review," *J. Struct. Eng.* 137(10), 1085-1095. DOI: 10.1061/(ASCE)ST.1943-541X.0000353

Article submitted: March 20, 2018; Peer review completed: May 13, 2018; Revisions accepted: June 14, 2018; Published: June 15, 2018.
DOI: 10.15376/biores.13.3.6021-6032